Hindawi
Shock and Vibration
Volume 2021, Article ID 2573201, 14 pages
https://doi.org/10.1155/2021/2573201

Research Article

Safety Assessment of Ancient Buildings under Adjacent Subway Blasting Construction Based on the Optimized Fuzzy Optimal Method

Bo Wu,[1,2,3] **Pingting Liu**,[1] **Wei Huang**,[1] **and Guowang Meng**[1]

[1]*College of Civil Engineering and Architecture, Guangxi University, Nanning, Guangxi 530004, China*
[2]*School of Civil and Architectural Engineering, East China University of Technology, Nanchang, 330013 Jiangxi, China*
[3]*School of Architectural Engineering, Guangzhou City Construction College, Guangzhou, Guangdong 510925, China*

Correspondence should be addressed to Wei Huang; wei.huang.edu@gmail.com

Received 16 April 2021; Revised 3 July 2021; Accepted 23 October 2021; Published 8 November 2021

Academic Editor: Xiaowei Deng

Fragile ancient buildings are recognized as an eloquent testimony to human civilization, and their safety should arouse more attention. According to the special case of adjacent blasting construction, the assessment model should be essentially built to assess the effect of tunnel blasting on the safety of the ancient buildings. To analyze the structural safety of ancient buildings under blasting vibration and to protect the precious ancient buildings, a risk assessment model of ancient buildings with 20 relevant assessment indexes was initiatively built in this study. To be specific, the relative factors of blasting, the factors of ancient buildings, and other factors (e.g., religion) were comprehensively considered in the model. Subsequently, the risk level and weight were calculated more systematically and quantitatively by adopting the optimized optimal comprehensive method integrating the G1 method and the entropy method. Lastly, the overall risk value was determined by applying the fuzzy gray method. Afterward, the value was adopted to assess the safety of the Asoka Temple, the only existing temple named after the Indian King Asoka in China, as an attempt to verify the feasibility of this model. Besides, the Asoka tunnel was around it. As demonstrated from the results, the age of the buildings maximally impacted the safety of ancient buildings, and the safety level of the Asoka Temple was "relatively safe." The present study built an effective model to assess the safety of ancient buildings under adjacent subway blasting construction, which could help improve the efficiency and accuracy of assessments.

1. Introduction

Ancient buildings are an eloquent testimony to the countries' history and the embodiment of the countries' culture. However, the safety and durability of the structures as well as the sensitivity to blasting of tunnel construction are decreasing with the aging of the buildings [1–3]. A reasonable safety assessment model should be built to assess the safety of ancient buildings and protect the ancient buildings from destruction. In this study, its own factors, the effect of vibration, and other factors (e.g., religion) were all considered to define the safety of ancient buildings to be no longer limited to safety of the structure, whereas a comprehensive safety assessment was conducted.

Over the past few years, the analysis of ancient building structures has aroused huge attention from numerous researchers. Structural damage correlated with ancient buildings [4–10] has been extensively investigated, and ancient buildings [11–13] have been monitored and measured. Moreover, Xue et al. built an earthquake damage assessment model for Chinese ancient wooden structures to reveal the influences exerted by the vibration on the ancient building [14]. Qiu et al. examined the effect of vibration attributed to Xi'an subway during the tunnel excavation on Xi'an ancient circumvallation [15]. Thus, the architectural factor should be considered in the risk assessment. Wang et al. built a prioritization model for historic building conservation by complying with object element theory and then proposed a novel assessment decision method for subsequent heritage impacts following the metro lines [4]. Though the building structure has been extensively studied, most of the existing studies had certain limitations. To be specific, the safety of ancient buildings was only studied from a single perspective (e.g., vibration or structure). As indicated from the literature review, other factors (e.g., the public religious sentiment) should be considered when assessing the safety of ancient buildings [16]. Accordingly, a novel and comprehensive assessment model should be built given the factors of ancient buildings and the effect of other disciplines.

According to engineering, risks are estimated by adopting some methods. Lu et al. [17] exploited the fuzzy COPRAS (complex proportional assessment) method to select the optimal green suppliers. Besides, the cross-entropy optimization model was adopted to objectively determine the weight vector, and a mathematical programming model of dual-objective probabilistic neural network was built to obtain the comprehensive attribute weights of two inconsistent indicators. The model was verified to be effective by conducting an example study. The entropy method was generally adopted for decision making. Furthermore, the G1 method is considered an optimized AHP method without the requirement for a consistency test. Though various studies have long been conducted on the risk analysis of ancient buildings, few researchers have comprehensively considered the factors and built an assessment model in numerous aspects. Accordingly, the optimal combination weighting method of entropy value method integrated with the G1 method could make the assessment more accurate and more effectively control the risk of ancient buildings as a whole.

It is noteworthy that the Asoka Temple was taken as an example to verify and practically implement the model built by using the optimal weighting method, and the results were consistent with the relevant engineering practice. The mentioned assessment system based on the optimized fuzzy optimal method could effectively identify and reasonably assess the safety of ancient buildings, which showed the guiding significance to the subsequent protection of the ancient buildings.

2. Methodology

The steps shown in Figure 1 were followed to assess the safety of the ancient building and optimize the risk assessment [18].

According to the mentioned steps, the safety assessment can be presented in Figure 2. The specific risk assessment is illustrated in Figure 3.

2.1. Basic Principle

2.1.1. G1 Method and Its Improvement. In fact, the G1 method (order relation analysis method) [19] refers to a type of order relation analysis method without the requirement for a consistency test, thereby leading to a decrease in the computational complexity and an increase in the computation efficiency. The steps of the G1method (Figure 2) are as follows [19]:

(1) Determine the order relationship between the assessment indexes X_m:

$$X_1 > X_2 > \cdots > X_{k-1} > X_k > \cdots > X_m. \quad (1)$$

(2) Judge the relative significance between the adjacent index:

$$r_k = \frac{w_{k-1}}{w_k}, \quad k = m, m-1, m-2, \ldots, 3, 2, \quad (2)$$

where r_k denotes the coefficient of significance of X_{k-1} to X_k.

(3) The calculation of the weighting number:

$$w_n = \left[1 + \sum_{k=2}^{n}\left(\prod_{j=k}^{n} r_j\right)\right]^{-1}. \quad (3)$$

The weight matrix of the index $X = \{X_1, X_2, \ldots, X_m\}$:

$$W = \begin{bmatrix} w_1 & w_2 & \cdots & w_n \end{bmatrix}^T. \quad (4)$$

As impacted by the limitation of human cognition and the complexity of the risk problem, experts failed to accurately determine the specific order of the weight while providing the exact degree of the significance coefficient. Thus, the redefinition of the weight calculation coefficient was adopted during the calculation. Since the significance score recommended in the Guidelines [20] optimizes the significance comparison method, a significance assessment standard for the G1 method was proposed in this study, and experts were invited to compare the materiality of the respective risk indicator on a case-by-case basis. The novel expert scoring criteria [21] are listed in Table 1.

2.1.2. Entropy Weight Method. To avoid the subjectivity of the results, an objective weighting method should be comprehensively selected. The entropy weight method [22, 23] has been extensively applied in problem decision making and exhibits strong objectivity. The entropy weight method was applied to the weight calculation to reduce the subjectivity brought by expert grading according to the G1 method. It could determine the weight of relevant factors by analyzing the amount of the information entropy of the respective indicator value [24, 25]. The smaller the information entropy is, the greater the weight of the indicator would be. However, the subjective intention of the decision maker could be easy to ignore. The risk fell to five levels based on ISO 31000 [20]. The risk scale is illustrated in Figure 4.

Risk assessment criteria were formulated in accordance with the relevant codes [20, 26–31] and in consultation with experts in special fields. The experts invited consisted of researchers in the protection of ancient buildings, architectural protection engineers, government regulators, tunnel

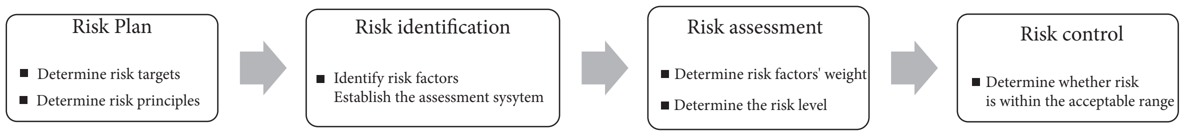

FIGURE 1: Risk management steps.

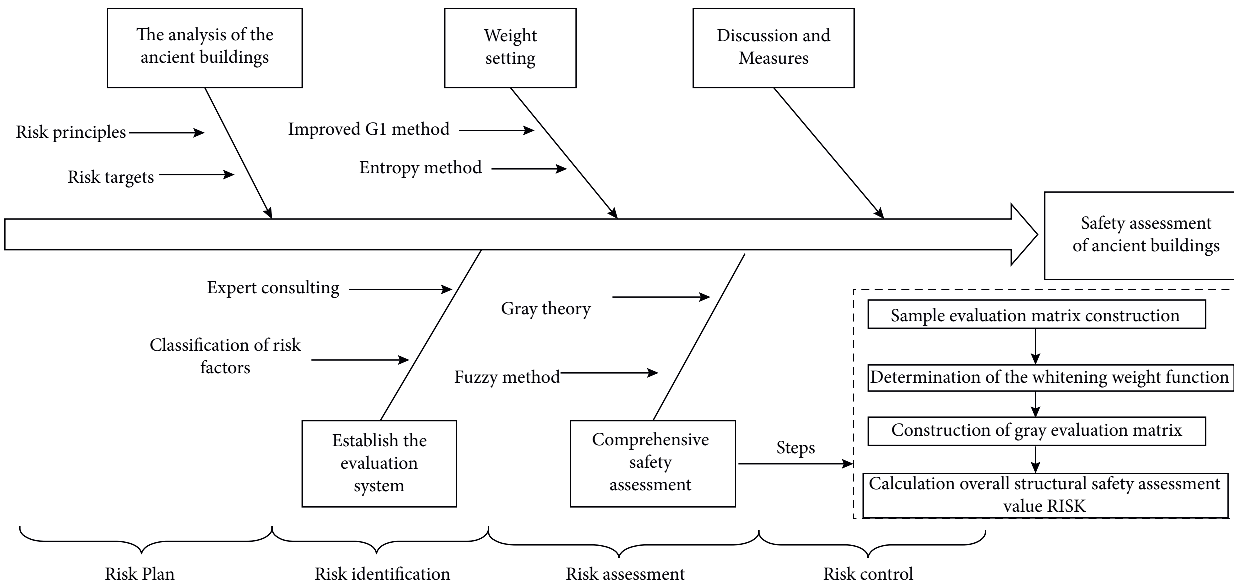

FIGURE 2: Safety assessment process.

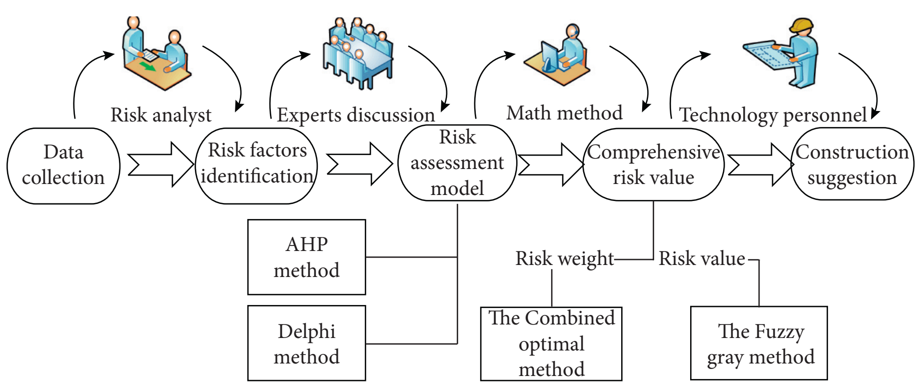

FIGURE 3: Specific process.

TABLE 1: Expert scoring criteria of the significance.

The degree of significance	Score
Particularly important	9-10
Comparatively important	6–8
Important	4-5
Unimportant	1–3

engineers, and tunnel technicians, who had high professional levels and huge engineering experiences and were in expert assessment teams. Subsequently, experts rated risk factors by complying with the criteria and actual situation of ancient buildings. The resulting risk scores were regarded as the entropy of each factor. In this study, the node value of risk classification and the data under the assessment of object indicators could jointly constitute the original indicator data. Afterward, the entropy value method could process the data to determine the ranking of the significance of the indicators. The specific steps are illustrated in Figure 2.

2.2. Assessment System Establishment

2.2.1. Establishment of the System. In the present study, the factors (e.g., ancient buildings and blasting vibration) were considered with the references of Chinese regulations on ancient buildings and relevant literature to build the safety

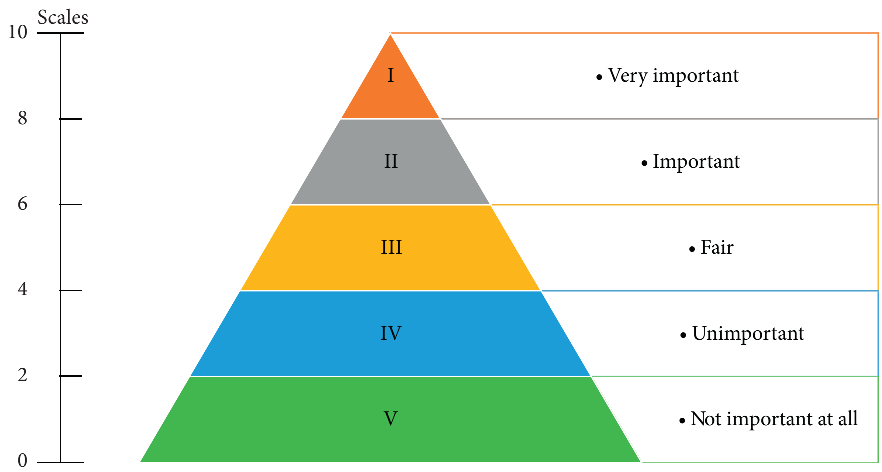

FIGURE 4: Risk scales.

and risk assessment system of ancient buildings. To be specific, the developed risk system consisted of three floors. The first floor was the risk of ancient buildings U. The second target floor was composed of the building factors U_1, blasting vibration factors U_2, and other factors U_3.

Given the literature review [5, 7, 11–13], this study subdivided the risk of ancient buildings into three target floors. U_1 contained nine subfactors, U_2 consisted of seven subfactors, and U_3 covered four subfactors. The system is presented in Figure 5.

Table 2 lists the risk assessment criteria of the ancient buildings corresponding to risk factors in Figure 5. U_{11} (foundation type), U_{12} (age of the buildings), U_{13} (significance), and U_{14} (materials) represent the durability of the foundation of ancient buildings, the time of building the buildings, the protection level of the buildings in accordance with the national cultural relic classification standard, and the materials adopted to construct ancient buildings, respectively. U_{15} (durability), U_{16} (height), and U_{17} (size), respectively, denote the durability of ancient buildings, the height of the buildings, and the floor space of the ancient buildings. U_{18} (structure safety level) refers to the safety level of the ancient buildings assessed by the code [29]. Besides, U_{19} (velocity response) represents the gap between the velocity response and permissible velocity of vibration [30]. U_{21} (vibration source type), U_{22} (frequency range), U_{23} (source distribution), U_{24} (blasting methods), U_{25} (propagation velocity of an elastic wave), U_{26} (position between buildings and source), and U_{27} (distance between buildings and source), respectively, denote the cause of the vibration, the frequency exhibited by the blast, the type of blasting source distribution, the method rationality, the propagation velocity of an elastic wave, the position between buildings and source, and the distance between buildings and source. Furthermore, U_{31} (construction personnel management), U_{32} (public religious sentiment), U_{33} (engineering geological condition), and U_{34} (engineering hydrologic condition), respectively, represent the management during the construction, the public awareness and the degree of piety, the engineering geological condition, and the engineering

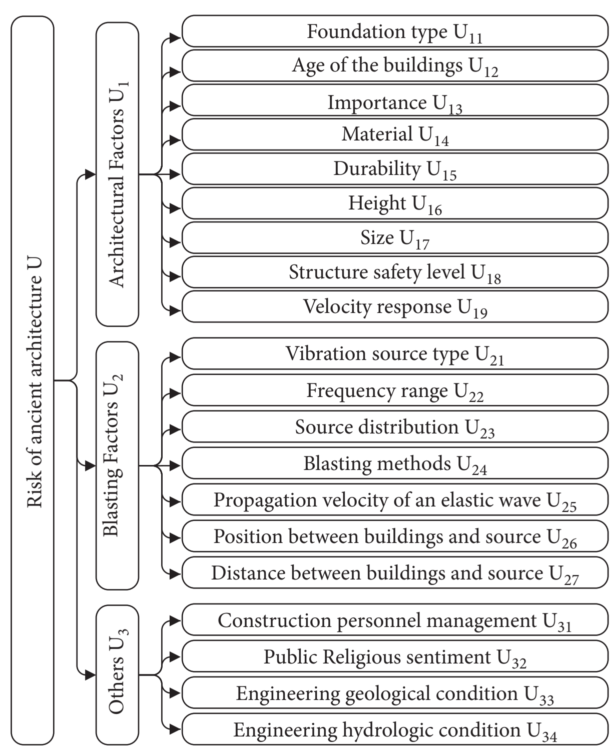

FIGURE 5: The risk assessment system.

hydrologic condition. A hierarchical assessment system was established, and the model fell to three levels. The correlation between the upper and lower levels was summarized and listed.

2.3. Weight Setting

2.3.1. Combination Weighting Method. The combined weighting method [32] could indicate the opinions and preferences of decision makers, as well as the laws of objective data. Besides, the difference between subjective weight and objective weight complied with the difference

Table 2: The score criteria of the risk.

	0~2 (V)	2~4 (IV)	4~6 (III)	6~8 (II)	8~10 (I)
U_{11}	Stable	Relatively stable	Relatively fragile	Fragile	Extremely fragile
U_{12}	The Old Stone Age	The Neolithic Age	Ancient times		Modern times
U_{13}	National level	Provincial level	City level	County level	Township level
U_{14}	Grotto structure	Brick masonry structure	Masonry-timber structure	Stone structure	Timber structure
U_{15}	Good durability	Relatively good durability	Relatively bad durability	Bad durability	Extremely bad durability
U_{16}	>25 m	20–25 m	15–20 m	10–15 m	<10 m
U_{17}	>100000 m^2	10000–100000 m^2	1000–10000 m^2	100–1000 m^2	<100 m^2
U_{18}	4th level	3rd level		2nd level	1st level
U_{19}	Much larger	Larger	Approximately equal	Less	Much less
U_{21}	Dynamic compaction	Piling	Cars, city trains	Subway	Train
U_{22}	<4 Hz	4-7 Hz	7–110 Hz	10–13 Hz	>13 Hz
U_{23}	Concentrated	Relatively concentrated	Relatively sporadic	Sporadic	Extremely sporadic
U_{24}	Reasonable	Relatively reasonable	Relatively unreasonable	Unreasonable	Extremely unreasonable
U_{25}	1500 m/s	2100–1500 m/s	2900–2100 m/s	5600–2900 m/s	>5600 m/s
U_{26}	Underground			Overground	
U_{27}	<100 m	100–400 m	400–700 m	700–1000 m	>1000 m
U_{31}	Strict	Relatively strict	General	Relatively free	Free
U_{32}	Strong	Relatively strong	General	Relatively weak	Weak
U_{33}	Strong	Relatively strong	General	Relatively weak	Weak
U_{34}	Strong	Relatively strong	General	Relatively weak	Weak

between their corresponding distribution coefficients. The combination coefficient of subjective factors and objective factors was determined by equations (5)–(10) to yield the combination weight. Subjective weighting was determined by consulting the opinions of relevant experts, followed by the entropy according to statistics. The optimal combination weighting model was built to address the unreasonable weight problem of single weighting. The steps to obtain the combined weight are illustrated in Figure 6.

The combination weight method should determine the combination weight coefficient in accordance with the following two factors.

The first was to ensure the minimum distance between the weighted score of each assessment object and the ideal generalized point in the following formula.

$$\min \sum_{i=1}^{n} l_i = \sum_{i=1}^{n}\sum_{j=1}^{m}\sum_{c=1}^{s} \alpha_c w_j^c \left(1 - v_{ij}\right). \tag{5}$$

The second was Jaynes maximum entropy principle [7], capable of avoiding the contribution error of various weighting results to the combined weighting results to the maximal extent.

The objective function built by the idea of minimizing the difference of the respective weighting result could simplify the calculation:

$$\max Z = -\sum_{c=1}^{s} \alpha_c \ln \alpha_c, \tag{6}$$

$$\begin{aligned} &\min \theta \sum_{i=1}^{n}\sum_{j=1}^{m}\sum_{c=1}^{s} \alpha_c w_j^c \left(1 - v_{ij}\right) + \left(1 - \theta \sum_{c=1}^{s} \alpha_c \ln \alpha_c\right), \\ &\text{s.t.} \sum_{c=1}^{s} \alpha_c = 1, \quad v_c \geq 0, \end{aligned} \tag{7}$$

where α denotes the balance coefficient between the two targets, $0 \leq \theta \leq 1$, $\theta = 0.5$. Given the mentioned two factors, the Lagrange function could yield the combination weight coefficient and the value of α_c:

$$\alpha_c = \frac{\exp\left\{-\left[1 + \theta \sum_{i=1}^{n} \sum_{j=1}^{m} w_j^c \left(1 - v_{ij}\right) / (1 - \theta)\right]\right\}}{\sum_{i=1}^{s} \exp\left\{-\left[1 + \theta \sum_{i=1}^{n} \sum_{j=1}^{m} w_j^c \left(1 - v_{ij}\right) / (1 - \theta)\right]\right\}}. \tag{8}$$

The combination weight w [32]:

$$w = \sum_{c=1}^{s} \alpha_c w_c, \tag{9}$$

where w_c represents the weight of the index obtained by a single method.

$$\sum_{c=1}^{s} \alpha_c = 1. \tag{10}$$

2.4. Comprehensive Safety Assessment

2.4.1. Gray Fuzzy Analysis Method. By using the gray fuzzy assessment method to the risk assessment of ancient buildings, the cognitive differences attributed to evaluators could be avoided to a certain extent, and the scientific nature of the assessment results could be improved. The process of the gray theory [33, 34] calculation (sample assessment matrix construction ⟶ determination of the whitening weight function ⟶ construction of gray assessment matrix), the whitening weight function, and gray assessment matrix were acquired by the following equations [35].

(1) Sample Assessment Matrix Construction. The risk assessment level vector can be acquired based on the established risk assessment indicators system:

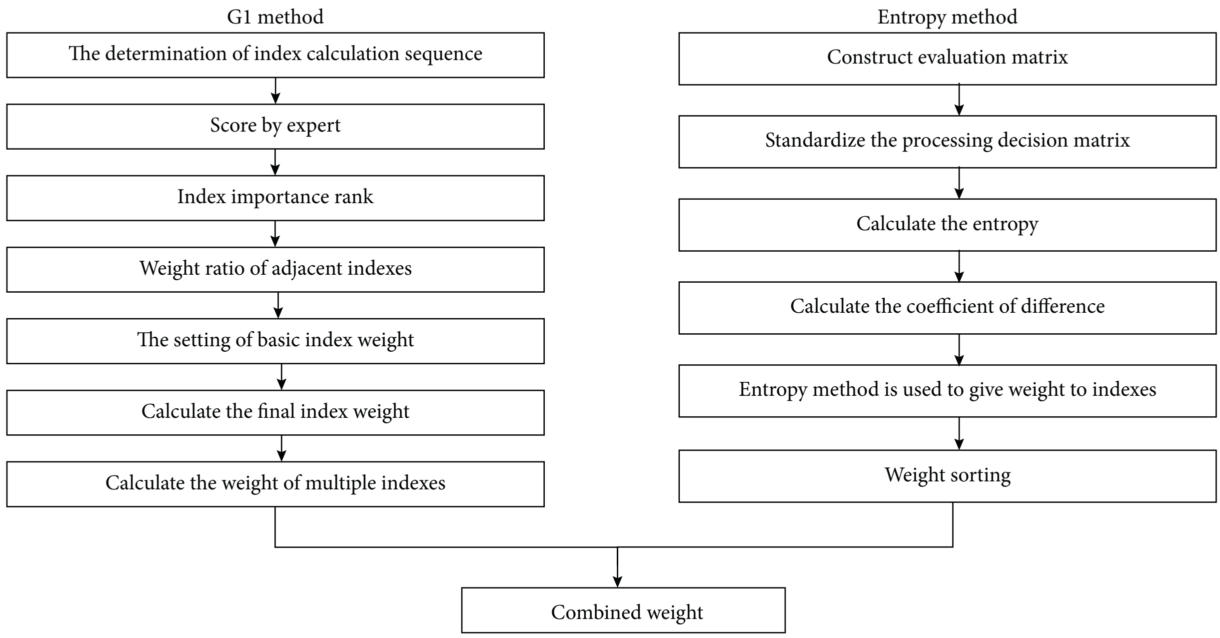

Figure 6: Combined weight steps.

$$V = (v_1, v_2, v_3, \ldots, v_t), \tag{11}$$

where t represents the number of risk levels. By using the Delphi method [21], p experts invited independently scored the respective indicator with the consideration of the assessment level vector V. Set the jth expert's assessment value of the jth secondary indicator of the first-level indicator U_i of the criterion level as $d_{ij}^{(q)}$. The final sample assessment matrix D obtained is written as

$$D = \begin{bmatrix} d_{11}^{(1)} & d_{12}^{(1)} & \cdots & d_{ij}^{(1)} & \cdots & d_{nn_i}^{(1)} \\ d_{11}^{(2)} & d_{12}^{(2)} & \cdots & d_{ij}^{(2)} & \cdots & d_{mn_i}^{(2)} \\ \vdots & \vdots & & \vdots & & \vdots \\ d_{11}^{(q)} & d_{12}^{(q)} & \cdots & d_{ij}^{(q)} & \cdots & d_{mn_i}^{(q)} \\ \vdots & \vdots & & \vdots & & \vdots \\ d_{11}^{(p)} & d_{12}^{(p)} & \cdots & d_{ij}^{(p)} & \cdots & d_{mn_i}^{(p)} \end{bmatrix}, \tag{12}$$

where $i = 1, 2, 3, \ldots, n$; $j = 1, 2, 3, \ldots, n$; i, $q = 1, 2, \ldots, p$;

(2) Determination of the Whitening Weight Function. The determination of the whitening function was different due to the different assessment objects. The function used in the gray assessment method was determined abiding by the literature and the practical assessment of this study. In the present study, the risk fell to five levels. Thus, we chose the five gray assessment model [36]. The functions that can be used to construct the gray assessment matrix in the gray statistical method are listed in Table 3.

(3) Construction of Gray Assessment Matrix. It can be assumed that there are E gray classes. The whitening weight functions f_e were determined by the gray statistics method. Subsequently, the whitening weights of the assessment sample $d_{ij}^{(q)}$ pertaining to the e ($e = 1, 2, 3, \ldots, E$) gray classes were calculated. E of the gray class of the whitening weights was f_e $(d_{ij}^{(q)})$.

The following equations represent the gray statistics $n_{ij}^{(e)}$ of the index U_{ij} pertaining to the eth gray class and the total gray statistics n_{ij}, respectively [36]:

$$\begin{aligned} n_{ij}^{(e)} &= \sum_{q=1}^{p} f_e\left(d_{ij}^{(q)}\right), \\ n_{ij} &= \sum_{e=1}^{E} n_{ij}^{(e)}. \end{aligned} \tag{13}$$

Based on the gray statistics and the total gray statistics, the gray assessment weight $z_{ij}^{(e)}$ could be calculated by

$$z_{ij}^{(e)} = \frac{n_{ij}^{(e)}}{n_{ij}}. \tag{14}$$

In the above equation, the value of $z_{ij}^{(e)}$ indicates how strongly all experts advocate that U_{ij} belongs to the eth gray class. The gray assessment weight vector $Z_i = (z_{ij}^{(1)}, z_{ij}^{(2)}, \ldots, z_{ij}^{(e)}, \ldots, z_{ij}^{(E)})$ of U_{ij} for each assessment gray class can be obtained from $z_{ij}^{(e)}$. In turn, the gray assessment matrix Z of indicator U_{ij} on each assessment gray class is expressed as

$$Z = \begin{bmatrix} Z_1 \\ Z_2 \\ \vdots \\ Z_i \\ \vdots \\ Z_n \end{bmatrix} = \begin{bmatrix} z_{11}^{(1)} & z_{11}^{(2)} & \cdots & z_{11}^{(e)} & \cdots & z_{11}^{(E)} \\ z_{12}^{(1)} & z_{12}^{(2)} & \cdots & z_{12}^{(e)} & \cdots & z_{12}^{(E)} \\ \vdots & \vdots & \vdots & \vdots & \vdots & \vdots \\ z_{ij}^{(1)} & z_{ij}^{(2)} & \cdots & z_{ij}^{(e)} & \cdots & z_{ij}^{(E)} \\ \vdots & \vdots & \vdots & \vdots & \vdots & \vdots \\ z_{nn_i}^{(1)} & z_{nn_i}^{(2)} & \cdots & z_{nn_i}^{(e)} & \cdots & z_{nn_i}^{(E)} \end{bmatrix} \quad i = 1, 2, \ldots, E. \tag{15}$$

Table 3: Gray whitening weight function.

The gray class	Level	e	Function
The first gray class	Safe	1	$f_{e=1}(v_{ij}) = \begin{cases} v_{ij}/9 & v_{ij} \in [0,9) \\ 1 & v_{ij} \in [9,10] \end{cases}$
The second gray class	Relatively safe	2	$f_{e=2}(v_{ij}) = \begin{cases} v_{ij}/7 & v_{ij} \in [0,7) \\ 2 - v_{ij}/7 & v_{ij} \in [7,10] \end{cases}$
The third gray class	Relatively dangerous	3	$f_{e=3}(v_{ij}) = \begin{cases} v_{ij}/5 & v_{ij} \in [0,5) \\ 2 - v_{ij}/5 & v_{ij} \in [5,10] \\ 0 & v_{ij} \notin [5,10] \end{cases}$
The fourth gray class	Dangerous	4	$f_{e=4}(v_{ij}) = \begin{cases} v_{ij}/3 & v_{ij} \in [0,3) \\ 2 - v_{ij}/3 & v_{ij} \in [5,6] \\ 0 & v_{ij} \notin [5,6] \end{cases}$
The fifth gray class	Extremely dangerous	5	$f_{e=5}(v_{ij}) = \begin{cases} 1 & v_{ij} \in [0,1) \\ 2 - v_{ij} & v_{ij} \in [1,2] \\ 0 & v_{ij} \notin [2,10] \end{cases}$

2.4.2. Gray Relation Sensitivity Analysis. The advantage of gray relational degree analysis is that it can be easy to calculate, and there will be no inconsistency between the quantitative results and the qualitative results. The calculated steps are represented as follows.

(1) Prioritization: m represents the number of assessment samples; n represents risk assessment index; $\overline{x_i}$ is the mean value of the index set; and x_0 is the reference sample. We set it as the final risk in the gray fuzzy method in this article. The original assessment matrix x_i' is [37]

$$x_i' = \left\{x\prime(1), x'(2), \ldots, x\prime(m)\right\},$$
$$x_i = \left\{\frac{x_i(1)}{\overline{x_i}}, \frac{x_i(2)}{\overline{x_i}}, \ldots, \frac{x_i(m)}{\overline{x_i}}\right\}, \tag{16}$$

where $i = 0, 1, 2, \ldots, n$.

(2) Absolute difference $\Delta_i(k)$ calculation:

$$\Delta_i(k) = \left|x_0(k) - x_i(k)\right|, \tag{17}$$

where $k = 0, 1, 2, \ldots, m$.

(3) Calculation of correlation coefficient $\zeta_i(k)$:

$$\zeta_i(k) = \frac{\Delta_{\min} + \rho\Delta_{\max}}{\Delta_i(k) + \rho\Delta_{\max}}, \tag{18}$$

where $\rho = 0.5$.

(4) Gray correlation r_i calculation:

$$r_i = \frac{1}{m}\sum_{k=1}^{m}\zeta_i(k). \tag{19}$$

The greater the correlation is, the weaker the uncertainty and the less the sensitivity would be.

2.4.3. Comprehensive Assessment. Based on the weight vector W and the gray assessment matrix Z obtained by the optimized combination method and the gray statistical method, respectively, their product was the comprehensive assessment vector H [24]:

$$H = W * Z. \tag{20}$$

Under the combination of the integrated assessment vector H and the risk level vector V, the overall structural safety assessment value risk of the system was the product of the H and the risk level vector V:

$$\text{Risk} = H * V^T. \tag{21}$$

During the practical assessment process, the most intuitive way was to express the risk status of the system as quantitative assessment values. *Risk* denotes the final risk assessment value of the system. The safety risk level of the system could be determined through the combination with the risk assessment level vector V. It laid a scientific and effective reference basis for assessing the safety of ancient building structures.

3. A Case Study

3.1. The Study Area. The Asoka Temple was initially established in the third year of Taikang emperor of the Western Jin Dynasty (282 AD) with a history of over 1,700 years, located in Yinzhou District of Ningbo. The Asoka Temple is known as the "Southeast Buddhist country." It refers to famous 283 temples of Zen Buddhism and one of the Chinese Buddhism "five mountains." Moreover, it is the only existing thousand-year-old temple in China named after the Indian King Asoka. The temple is notable for its treasure of Sakyamuni Buddha and exquisite pagoda. There are numerous scenic spots and historical sites close to King Asoka Temple. The plan is presented in Figure 7. The Asoka Temple takes up a crucial position to inherit the favorable Buddhist cultural tradition and carry forward the Buddhist cultural thoughts in the history of Buddhism for its historical and cultural value.

Given the urban transportation planning, the Treasure House Station of the Ningbo rail transit 1st line 2nd phase

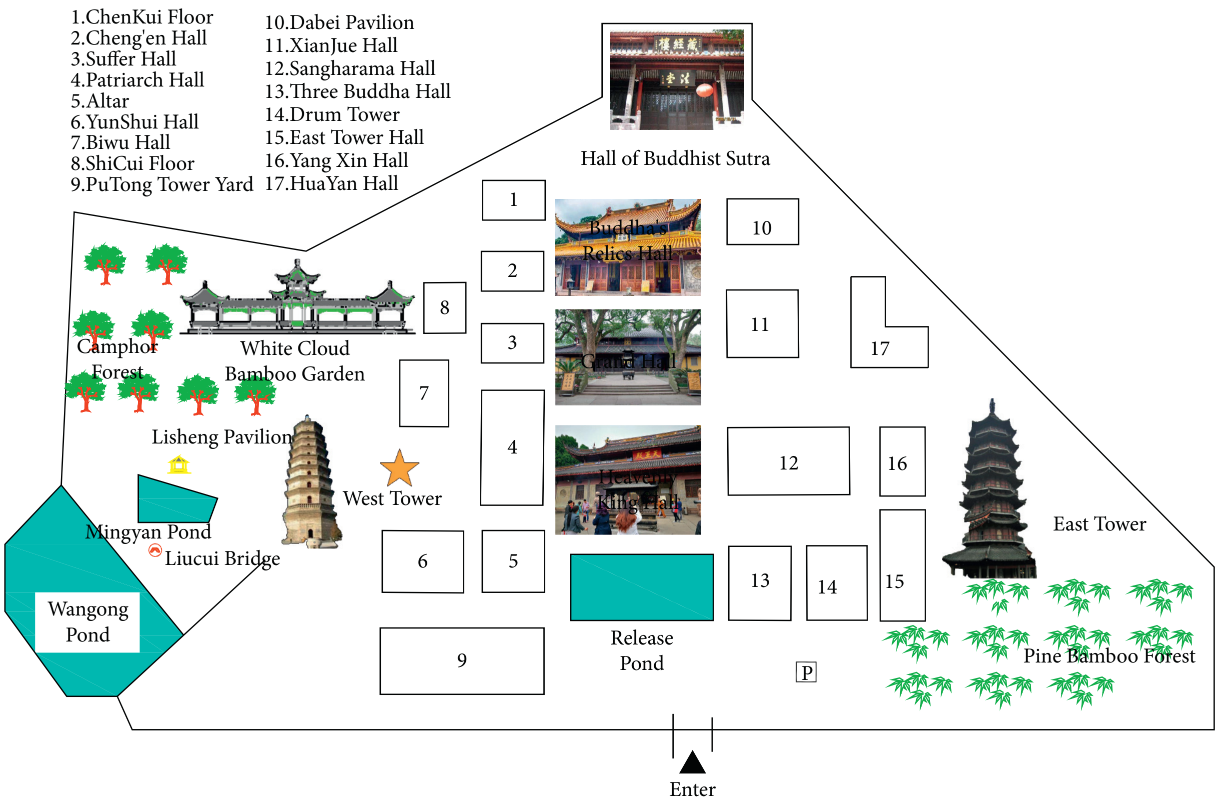

Figure 7: The plan of the Asoka Temple.

went through the Asoka Temple. The Asoka tunnel refers to the only tunnel project in Ningbo with drilling and blasting construction methods. The construction of the tunnel went through the fault fracture zone. Moreover, the surrounding environment of this tunnel is complex. The upper soil slope section exhibits poor stability. Several parts of the tunnel exit are made up of gravel silty clay, intensely weathered rhyolite porphyry, moderately weathered rhyolite porphyry, and fault fracture zone. The rock mass was relatively cracked and underwent strong weathering. This project exhibits poor self-steady ability. The core protection area of Asoka Temple, a national-level cultural relic protection unit, is approximately 98.6 m away from the tunnel. Figure 8 illustrates the relative position between the subway and the temple. Thus, blasting vibration is capable of easily affecting the safety of the Asoka Temple and the stability of the existing railways. A safety assessment is required for the Asoka Temple.

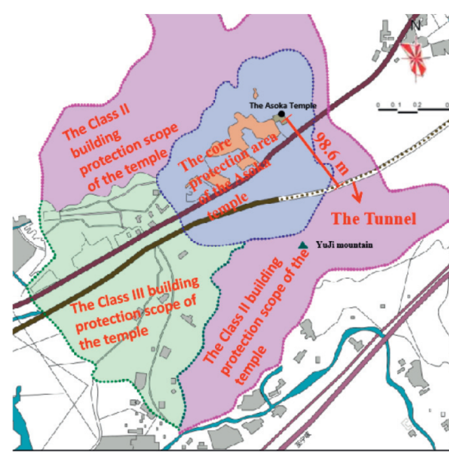

Figure 8: The location map of the Asoka Temple.

3.2. *The Weight Results and Analysis*

3.2.1. G1 Methods. Ten experts were invited to fill in the scoring form in Table 4. Experts scored the significance of risk indicators abiding by the criteria in Table 1.

The weight obtained by the subjective assessment method of the first index and the secondary index is listed in Table 5.

Table 4: Expert scores.

Indicators	A_1	A_2	...	A_m
Score	$X_{A_{1J}}$	$X_{A_{2J}}$	...	$X_{A_{mJ}}$

3.2.2. Risk Factor Weight Values Determined Based on Entropy Weighting Method. Ten experts scored the 20 indicators by using the safety assessment system, as listed in Table 2. The score ranged from 1 to 10, with the most significance when reaching 10 and the least significance when reaching 1. Moreover, the weight calculation of the risk factors was performed with the improved order relation analysis method, and the results are listed in Table 6.

Table 5: Risk factor of G1 method.

	The 2nd indicator	The 2nd weight	The 3rd indicator	The 3rd weight	Total weight
U	U_1	0.4	U_{11}	0.15	0.06
			U_{12}	0.21	0.084
			U_{13}	0.08	0.032
			U_{14}	0.12	0.048
			U_{15}	0.11	0.044
			U_{16}	0.08	0.032
			U_{17}	0.05	0.02
			U_{18}	0.13	0.052
			U_{19}	0.07	0.028
	U_2	0.5	U_{21}	0.13	0.052
			U_{22}	0.15	0.06
			U_{23}	0.16	0.064
			U_{24}	0.18	0.072
			U_{25}	0.12	0.048
			U_{26}	0.11	0.044
			U_{27}	0.15	0.06
	U_3	0.1	U_{31}	0.32	0.032
			U_{32}	0.15	0.015
			U_{33}	0.32	0.032
			U_{34}	0.21	0.021

Table 6: Risk index weights of entropy weight method.

	The secondary indicators	Secondary index weight	Tertiary indicators	Tertiary index weight
U	U_1	0.562	U_{11}	0.17
			U_{12}	0.26
			U_{13}	0.07
			U_{14}	0.08
			U_{15}	0.11
			U_{16}	0.07
			U_{17}	0.06
			U_{18}	0.11
			U_{19}	0.07
	U_2	0.316	U_{21}	0.16
			U_{22}	0.13
			U_{23}	0.13
			U_{24}	0.16
			U_{25}	0.12
			U_{26}	0.12
			U_{27}	0.18
	U_3	0.122	U_{31}	0.35
			U_{32}	0.11
			U_{33}	0.32
			U_{34}	0.22

3.2.3. Optimal Assignment Weight Calculation. By normalizing the indicators, we obtained the combination coefficients with formula (5):

$$\alpha_c = (0.49, 0.51). \tag{22}$$

The calculation brought the weights of the indicators in the safety assessment system and the combination coefficients into the formula of the combination weights to obtain the combination weights. The results of combined weights are provided in Table 7.

3.3. Risk Values and Analysis. In fact, this study used the Delphi method and invited 10 experts to assess 18 risk indicators based on the score criteria in Table 1. Besides, the indicator matrix was constructed and then normalized. The results of experts' assessment of the risk indexes are shown in

Table 7: Combined weight.

Indicators	Entropy method weights	G1 method of weight	Combined weight
U_{11}	0.09554	0.06	0.0774146
U_{12}	0.14612	0.084	0.1144388
U_{13}	0.03934	0.032	0.0355966
U_{14}	0.04496	0.048	0.0465104
U_{15}	0.06182	0.044	0.0527318
U_{16}	0.03934	0.032	0.0355966
U_{17}	0.03372	0.02	0.0267228
U_{18}	0.06182	0.052	0.0568118
U_{19}	0.03934	0.028	0.0335566
U_{21}	0.05056	0.052	0.0512944
U_{22}	0.04108	0.06	0.0507292
U_{23}	0.04108	0.064	0.0527692
U_{24}	0.05056	0.072	0.0614944
U_{25}	0.03792	0.048	0.0430608
U_{26}	0.03792	0.044	0.0410208
U_{27}	0.05688	0.06	0.0584712
U_{31}	0.0427	0.032	0.037243
U_{32}	0.01342	0.015	0.0142258
U_{33}	0.03904	0.032	0.0354496
U_{34}	0.02684	0.021	0.0238616

Table 8, from which we can analyze the opinions of 10 experts on the mentioned indicators.

Fuzzy assessment matrix:

$$D_1 = \begin{vmatrix} 5.8 & 6.2 & 5.7 & 6.0 & 5.4 & 5.6 & 5.1 & 6.1 & 6.3 & 5.8 \\ 7.1 & 7.5 & 7 & 6.4 & 6.6 & 7.2 & 7.4 & 7 & 6.8 & 7.1 \\ 8.2 & 8.5 & 8 & 7.9 & 7.4 & 7.1 & 7.6 & 7.8 & 7.5 & 7.4 \\ 6.5 & 6.2 & 7 & 6.6 & 6.6 & 6.8 & 6.7 & 6.9 & 7.1 & 7 \\ 7.1 & 7.5 & 7 & 7.4 & 6.8 & 7.1 & 7.1 & 7.2 & 6.7 & 7.2 \\ 6.8 & 6.5 & 6.6 & 6.1 & 6.8 & 6.7 & 6.6 & 6.9 & 7.2 & 6.8 \\ 7.3 & 7 & 7.5 & 7.2 & 7 & 7.1 & 7.2 & 8 & 6.9 & 7.2 \\ 6.5 & 6.8 & 6.6 & 7.2 & 7.1 & 7 & 7.1 & 7.5 & 6.8 & 7 \\ 7.6 & 7.5 & 8 & 7.2 & 6 & 7.4 & 7.3 & 7.5 & 5.6 & 7.2 \end{vmatrix}. \quad (23)$$

According to Table 3, the gray assessment matrix weight vector can be calculated, and the total calculation results are shown in Table 9.

The correlation coefficient and ranking of risk factors are represented in Table 10.

Form a gray assessment matrix from gray assessment weight vectors Z and obtain the comprehensive assessment vector according to formula (11):

$$H = [\,0.2910 \;\; 0.3634 \;\; 0.2780 \;\; 0.0166 \;\; 0\,]. \quad (24)$$

The overall tunnel safety assessment level of the system from the equation:

$$\text{Risk} = H * V^T = 6.6025. \quad (25)$$

4. Results and Discussion

Given Table 7, the weight of each tertiary risk factor was ranked as follows: $U_{32} < U_{34} < U_{17} < U_{19} < U_{33} < U_{13} < U_{16} < U_{31} < U_{26} < U_{25} < U_{14} < U_{22} < U_{21} < U_{15} < U_{23} < U_{18} < U_{27} < U_{24} < U_{11} < U_{12}$. The weights of the secondary risk factors were ranked as $U_1 > U_2 > U_3$. As indicated from the weighting, the indicators of the ancient building itself exerted a critical effect on its safety assessment. According to Figure 9, among the mentioned tertiary risk indicators, the age of ancient buildings gained the maximal weight since the older the ancient buildings in China are, the more likely they would be damaged. Moreover, previous protective measures may not be sufficiently effective due to the limitations of science and technology, thereby significantly impacting the safety of the mentioned buildings. The arrangement of the correlation degree in Table 10 revealed that the risk

Table 8: Risk index matrix.

Indicators	E_1	E_2	E_3	E_4	E_5	E_6	E_7	E_8	E_9	E_{10}
U_{11}	5.8	6.2	5.7	6.0	5.4	5.6	5.1	6.1	6.3	5.8
U_{12}	7.1	7.5	7	6.4	6.6	7.2	7.4	7.0	6.8	7.1
U_{13}	8.2	8.5	8.0	7.9	7.4	7.1	7.6	7.8	7.5	7.4
U_{14}	4.1	4.4	4.3	4.5	4.1	4	4.2	4.2	4.3	4.5
U_{15}	7.1	7.5	7	7.4	6.8	7.1	7.1	7.2	6.7	7.2
U_{16}	6.8	6.5	6.6	6.1	6.8	6.7	6.6	6.9	7.2	6.8
U_{17}	6.1	6.2	6.1	6.0	6.1	6.5	6.1	6.5	6.3	6.4
U_{18}	6.5	6.8	6.6	7.2	7.1	7.0	7.1	7.5	6.8	7.0
U_{19}	6.1	6.0	5.5	5.4	5.6	6.2	6.1	6.0	5.6	5.5
U_{21}	6.0	6.1	6.4	5.8	5.7	5.5	5.4	6.5	6.1	6.0
U_{22}	7.1	7.6	7.5	7.2	6.8	6.9	7.4	7.2	7.1	6.8
U_{23}	4.1	4.2	4.1	4.0	4	4.3	4.5	4.1	4.1	4.5
U_{24}	6.5	6.4	6.5	6.0	6.2	6.5	6.6	6.4	6.2	6.0
U_{25}	4.1	4.5	4.3	4.4	4.5	5.0	5.1	4.8	4.4	4.6
U_{26}	8.5	8	8.1	7.6	7.6	8.0	8.2	7.8	7.7	7.5
U_{27}	7.1	7.5	7.4	7.3	7.0	7.1	7.2	7.1	7.0	7.5
U_{31}	6.5	6	6.1	5.6	6.5	6.4	5.8	6.7	6.8	6.4
U_{32}	4.5	4.4	5.0	5.1	5.3	4.5	4.1	5.2	5.1	5.6
U_{33}	7.2	7.1	5.4	6.5	7.1	7.3	7.0	5.1	7.0	7.2
U_{34}	6.5	6.1	6.2	5.8	5.1	6.4	6.0	5.5	5.3	6.0

E_i means expert i, $i = 1, 2, 3, \ldots, 10$.

Table 9: The total calculation results.

Risk indicators	Total gray statistics	Gray assessment matrix weight vector	The risk value
U_{11}	23.1301	(0.2786, 0.3582, 0.3632, 0, 0)	6.8308
U_{12}	23.5975	(0.3301, 0.4165, 0.2534, 0, 0)	7.1534
U_{13}	23.1200	(0.3720, 0.4325, 0.1955, 0, 0)	7.3530
U_{14}	28.099	(0.1685, 0.2165, 0.4086, 0.2064, 0)	5.6942
U_{15}	23.6086	(0.3346, 0.4206, 0.2448, 0, 0)	7.1796
U_{16}	23.5873	(0.3156, 0.4046, 0.2798, 0, 0)	7.0716
U_{17}	23.3622	(0.2963, 0.3810, 0.3227, 0, 0)	6.9472
U_{18}	23.6276	(0.3273, 0.4154, 0.2573, 0, 0)	7.1400
U_{19}	23.9297	(0.2693, 0.3463, 0.3510, 0.0334, 0)	6.7030
U_{21}	24.0873	(0.2745, 0.3173, 0.3861, 0.0221, 0)	6.6884
U_{22}	23.5642	(0.3376, 0.4213, 0.2411, 0, 0)	7.1930
U_{23}	25.0546	(0.3014, 0.3875, 0.2985, 0.0126, 0)	6.9554
U_{24}	28.8699	(0.2860, 0.3464, 0.3676, 0, 0)	6.8368
U_{25}	23.9758	(0.3022, 0.3867, 0.2903, 0.0208, 0)	6.9406
U_{26}	22.9778	(0.3820, 0.4352, 0.1828, 0, 0)	7.3984
U_{27}	23.5822	(0.3402, 0.4240, 0.2358, 0, 0)	7.2088
U_{31}	23.5892	(0.2958, 0.3803, 0.3154, 0.0085, 0)	6.9268
U_{32}	25.3669	(0.2138, 0.2748, 0.3642, 0.1472, 0)	6.1104
U_{33}	23.9819	(0.3100, 0.3932, 0.2760, 0.0208, 0)	6.9834
U_{34}	23.6854	(0.2823, 0.3630, 0.3546, 0, 0)	7.1312

Table 10: Correlation coefficient and ranking of risk factors.

Risk indicators	Correlation coefficient	Rank
U_{11}	0.67	15
U_{12}	0.9	5
U_{13}	0.87	6
U_{14}	0.51	18
U_{15}	0.93	2
U_{16}	0.86	7
U_{17}	0.75	12
U_{18}	0.91	4
U_{19}	0.69	14
U_{21}	0.74	13
U_{22}	0.92	3
U_{23}	0.35	20
U_{24}	0.81	10
U_{25}	0.41	19
U_{26}	0.85	9
U_{27}	0.94	1
U_{31}	0.78	11
U_{32}	0.59	17
U_{33}	0.86	8
U_{34}	0.63	16

assessment value was highly sensitive to the two factors U_{23} and U_{25}, and U_{23} was the most sensitive.

The weighting of risk indicators was calculated with the combined optimal method, which reduced subjectivity in the assessment process to some extent. In particular, the greater the weighting is, the more significant the effect of the method on the combined weight would be. According to the risk values of the individual risk factors obtained in Table 7 and the overall risk value acquired eventually, the risk level of the building was IV (relatively safe).

As indicated in Figure 10, most of the risk factors of this project were in IV (relatively safe)-V (safe) risk level. However, the risk level of U_{14}, the structure type, was III (relatively dangerous). The structure type of the building referred to a masonry-timber building's structure. On the whole, its destruction factor included wood corrosion, moth, and building deformation. The safety of ancient buildings in masonry-timber structures was reduced attributed to long-time physical action, chemical action, and seismic factors. Moreover, the main vibration frequency of field blasting earthquakes was largely distributed in the range of 10–70 Hz, as indicated from the field data of the project. The structural dynamic response and modal analysis of the masonry tower indicate that its natural frequency ranged from 1 to 10 Hz. Thus, the two might overlap in the low-frequency region. While the blasting vibration was attenuated with the distance, the frequency of vibration tended to be in a smaller range and even overlapped the natural frequency. Consequently, the structural resonance would be caused inevitably, and then the dynamic response would be amplified. Thus, the blasting method U_{24} and the frequency range U_{22} should be considered.

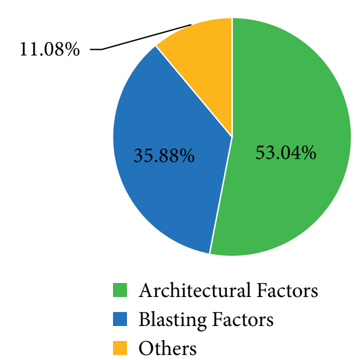

Figure 9: The combined risk weighting for ancient buildings.

In Figure 11, the range of most indicators' risk value was between 6 and 8, the fourth range according to Figure 4. It was therefore suggested that the experts invited considered

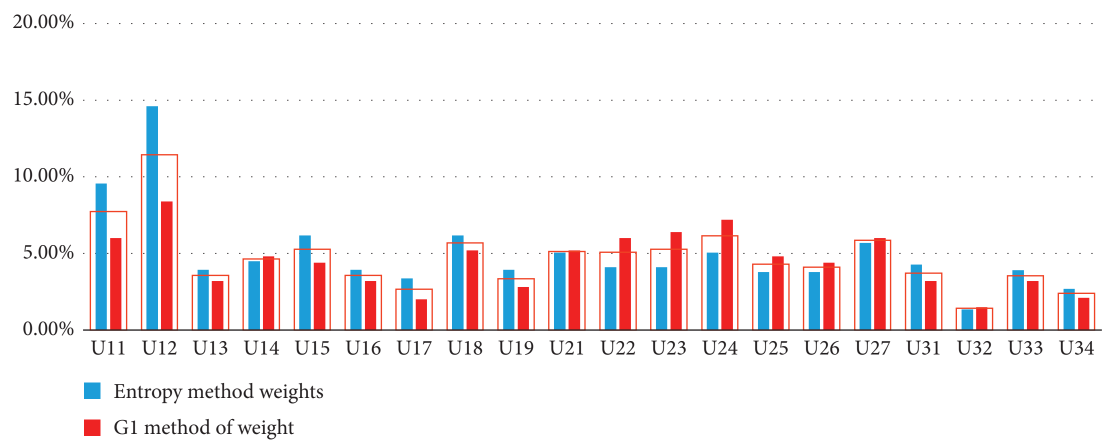

FIGURE 10: The combined risk weighting for ancient buildings.

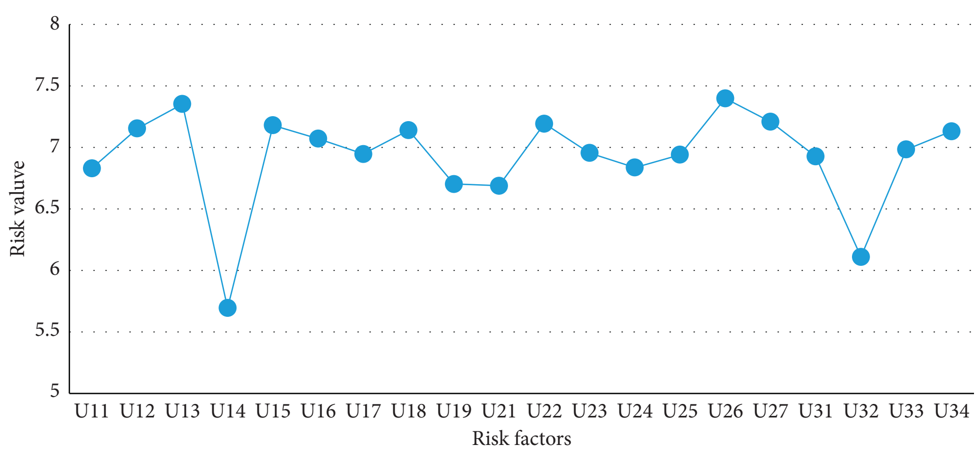

FIGURE 11: The risk values of risk indicators.

that the risk level of the mentioned factors was relatively safe given the situation provided by the actual engineering information. According to the mentioned results, dynamic blasting construction was adopted to monitor blast vibration. Such a method could maintain the security and durability of ancient buildings. Moreover, the step method, short drilling ruler method, and small dosage method were employed to regulate the risk factors according to the topographic and geological conditions of the site and the existing tunneling technology.

In the present study, the mean square root error (RMSE) acted as a convenient method to measure the deviation between the observed value and the true value. The synthetic risk value was taken as the observational value while the experts' score was considered true. As revealed from the results in Table 11, all relative errors were less than 1, thereby demonstrating that the model could be effective, which could be referenced for construction protection. Given the risk score of the expert assessment, the engineer should write the construction plan of safety protection of ancient buildings, and the constructor should take different

TABLE 11: The total calculation results.

Risk indicators	RMSE	Relative error
U_{11}	1.09	0.11
U_{12}	4.3	0.43
U_{13}	4.56	0.46
U_{14}	1.8	0.18
U_{15}	4.34	0.43
U_{16}	4.1	0.41
U_{17}	3.64	0.36
U_{18}	4.33	0.43
U_{19}	3.24	0.32
U_{21}	3.42	0.34
U_{22}	4.52	0.45
U_{23}	3.21	0.32
U_{24}	3.88	0.39
U_{25}	2.07	0.21
U_{26}	4.87	0.49
U_{27}	4.51	0.45
U_{31}	3.6	0.36
U_{32}	2.31	0.23
U_{33}	3.74	0.37
U_{34}	2.86	0.29

protective measures in accordance with the risk plan and obtain assessment results to increase the construction efficiency.

5. Conclusions

In this study, a set of safety assessment systems considering the complexity and fragility of ancient buildings was developed and applied to the Asoka Temple close to the Treasure House Station of Ningbo Rail Transit Line 1 Phase II Project. Several conclusions were drawn as follows:

(1) The present study improved the original G1 method and preprocessed the initial data obtained to comprehensively assess ancient buildings' safety. The method adopted here converted quantitative data into interval numbers. Compared with the conventional analytic hierarchy process, this method could be more reasonable and accurate. The results revealed the risk scores of the tunnel construction. Besides, the risk level of the respective risk factor was determined to target the risk factors in the construction and control the risk promptly. The algorithm could exert significant application effects on the risk assessment of ancient buildings through the calculation of an example.

(2) The safety assessment model exhibited generality and could be applied to other ancient buildings in the same situation. To a certain extent, this study could effectively protect the preservation of ancient buildings and facilitate the modernization of the country and the survival of ancient buildings. It is significant to maintain the historical culture and continuously develop the advanced multiculture.

(3) The optimized combined optimal method was employed to determine the weight of risk indicators and rank them given their significance. The results were real and reliable. The method guided the construction personnel to take appropriate protective measures. They could allocate protection resources timely and provide measures to construct target safety protection projects.

On the whole, this study expedited the optimization of the ancient building adjacent to the blasting safety assessment in China. It is noteworthy that this study still relied partially on the expert scoring method, so it was considered subjective. In the subsequent research, experts can exploit the fuzzy sets of images to assess the safety of ancient buildings qualitatively and quantitatively, achieve accurate and comprehensive assessment results, and then provide guidance opinions on the protection of the buildings. Furthermore, the combination of artificial neural networks and assessment methods can be employed to make the safety of buildings predictable.

Data Availability

The datasets employed and analyzed in the present study are available from the corresponding author upon reasonable request.

Conflicts of Interest

The authors declare that they have no conflicts of interest.

Acknowledgments

The authors would like to express their appreciation for the financial support from the National Natural Science Foundation of China (grant nos. 51678164 and 51478118), the Guangxi Natural Science Foundation Program (2018GXNSFDA138009), and the Guangxi Science and Technology Plan Projects (AD18126011).

References

[1] X. Li and D. Yuan, "Development of the safety control framework for shield tunneling in close proximity to the operational subway tunnels: case studies in mainland China," *SpringerPlus*, vol. 5, no. 1, p. 527, 2016.

[2] I. Ocak, "Environmental problems caused by Istanbul subway excavation and suggestions for remediation," *Environmental Geology*, vol. 58, no. 7, pp. 1557–1566, 2009.

[3] P. Liu, Q. Li, J. Bian, L. Song, and X. Xiahou, "Using interpretative structural modeling to identify critical success factors for safety management in subway construction: a China study," *International Journal of Environmental Research and Public Health*, vol. 15, no. 7, p. 1359, 2018.

[4] Q. Wang, C. Yang, J. Lu, F. Wu, and R. Xu, "Analysis of preservation priority of historic buildings along the subway based on matter-element model," *Journal of Cultural Heritage*, vol. 45, pp. 291–302, 2020.

[5] F. Clementi, A. Ferrante, E. Giordano, F. Lenci, and L. Stefano, "Damage assessment of ancient masonry churches stroked by the Central Italy earthquakes of 2016 by the non-smooth contact dynamics method," *Bulletin of Earthquake Engineering*, vol. 18, no. 2, pp. 455–486, 2020.

[6] L. Pecchioli, G. Marra, and M. Fabrizio, "Evidence of seismic damages on ancient Roman buildings at Ostia: an arch mechanics approach," *Journal of Archaeological Science: Report*, vol. 21, pp. 117–127, 2018.

[7] M. Valente, G. Biolzi, and B. Luigi, "Seismic assessment of two masonry Baroque churches damaged by the 2012 Emilia earthquake," *Engineering Failure Analysis*, vol. 79, pp. 773–802, 2017.

[8] G. Boscato and A. Cecchi, "Sensitivity analysis of geometric irregular effects on vulnerability of large-hall historic structures," *Engineering Failure Analysis*, vol. 115, 2020.

[9] R. Fanti, G. Gigli, L. Lombardi, D. Canuti, and C. Paolo, "Terrestrial laser scanning for rockfall stability analysis in the cultural heritage site of Pitigliano (Italy)," *Landslides*, vol. 10, no. 4, pp. 409–420, 2013.

[10] B. Jaishi, W.-X. Ren, Z.-H. Zong, and P. N. Maskey, "Dynamic and seismic performance of old multi-tiered temples in Nepal," *Engineering Structures*, vol. 25, no. 14, pp. 1827–1839, 2003.

[11] S. Invernizzi, G. Lacidogna, N. E. Carpinteri, and C. Alberto, "Structural monitoring and assessment of an ancient masonry tower," *Engineering Fracture Mechanics*, vol. 210, pp. 429–443, 2019.

[12] L. Fregonese, G. Barbieri, L. Biolzi, M. Bocciarelli, A. Frigeri, and L. Taffurelli, "Surveying and monitoring for vulnerability assessment of an ancient building," *Sensors*, vol. 13, no. 8, pp. 9747–9773, 2013.

[13] S. Coccia, M. Di Carlo, and D. C. Fabio, “Wind strength of Gothic cathedrals,” *Engineering Failure Analysis*, vol. 55, pp. 1–25, 2015.
[14] J. Y. Xue, Z. J. Wu, F. L. Zhang, and H. T. Zhao, “Seismic damage evaluation model of Chinese ancient timber buildings,” *Advances in Structural Engineering*, vol. 18, no. 10, pp. 1671–1683, 2015.
[15] J. Qiu, Y. Qin, Z. Feng, L. Wang, and K. Wang, “Safety risks and protection measures for city wall during construction and operation of xi’an metro,” *Journal of Technology*, vol. 34, no. 2, Article ID 04020003, 2020.
[16] F. Karaca, “An AHP-based indoor air pollution risk index method for cultural heritage collections,” *Journal of Cultural Heritage*, vol. 16, no. 3, pp. 352–360, 2015.
[17] J. Lu, S. Zhang, J. Wu, and Y. Wei, “Copras method for multiple attribute group decision making under picture fuzzy environment and their application to green supplier selection,” *Technological and Economic Development of Economy*, vol. 27, no. 2, pp. 369–385, 2021.
[18] J. Hao, J. Ren, Q. Wu et al., “Identifying factors associated with risk assessment competencies of public health emergency responders,” *International Journal of Environmental Research and Public Health*, vol. 14, no. 6, p. 597, 2017.
[19] Y. Guo, *The Theory and Method of Comprehensive Assessment*, Science Press, Beijing: China, 2002.
[20] Us-Ansi, *Risk Management—Principles and Guide-Lines*, Cerm Academy Serirs on Enterprise Risk Manage, Geneva, Switzerland, 2018.
[21] J. M. Soon, W. P. Davies, S. A. Chadd, and R. N. Baines, “A Delphi-based approach to developing and validating a farm food safety risk assessment tool by experts,” *Expert Systems with Applications*, vol. 39, no. 9, pp. 8325–8336, 2012.
[22] D. Zhao, H. Su, J. Wu, and J. Ma, “The wireless network security fuzzy risk assessment based on entropy theory,” *Computer application and software*, vol. 23, no. 8, pp. 24–26, 2006.
[23] G.-l. Xu, S.-P. Wan, and J.-Y. Dong, “An entropy-based method for probabilistic linguistic group decision making and its application of selecting car sharing platforms,” *Informatica*, vol. 31, no. 3, pp. 621–658, 2020.
[24] J. Y. Zhang and L. Z. Lei, “Fuzzy comprehensive evaluation method on water environmental quality based on entropy weight with consideration of toxicology of evaluation factors,” *Advanced Materials Research*, vol. 356-360, pp. 2383–2388, 2012.
[25] D. Wu, D. S. Tang, X. W. Yu, and Z. Y. Wen, “The application of entropy weight of attribute recognition model in reservoir eutrophication evaluation,” *Applied Mechanics and Materials*, vol. 477-478, pp. 870–873, 2014.
[26] State Bureau of Cultural Relics in China, *Specification for conservation and utilization of cultural heritage - Industrial Heritage*, State Cultural Relics Publishing House, Beijing, China, 2018.
[27] State Bureau of Cultural Relics in China, *Guideline for structural safety assessment of modern historic building*, Cultural Relics Publishing House, Beijing, China, 2014.
[28] State Bureau of Cultural Relics in China, *Specification for designing dossier of modern heritage building conservation project*, State Cultural Relics Publishing House, Beijing, China, 2017.
[29] State Forestry and Grassland Administration in China, *Technical code on appraisal rating for wooden member of ancient timber building*, Standards Press of China, Beijing, China, 2019.
[30] Ministry of Construction P.R. China, *Technical specifications for protection of historic buildings against man-made vibration*, China Architecture & Building Press, Beijing, China, 2008.
[31] State Bureau of Cultural Relics in China, *The code of construction supervision for relics building conservation project*, State Cultural Relics Publishing House, Beijing, China, 2012.
[32] B. He and L. Yin, “Optimal combined weight TOPSIS method for evaluating Internet resource abundance,” *Statistics & Decisions*, vol. 35, no. 18, pp. 36–40, 2019.
[33] Y. Jia, G. Li, X. Dong, and K. He, “A novel denoising method for vibration signal of hob spindle based on EEMD and grey theory,” *Measurement*, vol. 169, Article ID 108490, 2021.
[34] M.-F. Chen and G.-H. Tzeng, “Combining grey relation and TOPSIS concepts for selecting an expatriate host country,” *Mathematical and Computer Modelling*, vol. 40, no. 13, pp. 1473–1490, 2004.
[35] H. Jia, H. Jiang, J. Yu, J. Zhang, P. Cao, and X. Yu, “Total health expenditure and its driving factors in China: a gray theory analysis,” *Healthcare*, vol. 9, no. 2, p. 207, 2021.
[36] X. B. Ding, “The risk assessment of high-tech project based on comprehensive evaluation of fuzzy and gray model,” in *Proceedings of the 2nd International Conference on Sensors, Measurement and Intelligent Materials (ICSMIM 2013)*, pp. 1734–1737, PEOPLES R CHINA, Guangzhou, China, November 2013.
[37] Y. Desheng, *Grey theory and method*, Petroleum Industry Press, Beijing, China, 1992.